4. R. Lerch, Simulation of piezoelectric devices by two- and three-dimensional finite elements, IEEE Trans Ultrason Ferroelect Freq Cont 37 (1990), 233–247.
5. K.M. Lakin, Numerical analysis of two dimensional thin film resonators, IEEE Int Freq Cont Symp, Salt Lake City, USA (1993), 502–508.
6. K. Seo, S. Ju, and H. Kim, The modeling of thin-film bulk acoustic wave resonators using the FDTD method, IEEE Electron Device Lett 23 (2002), 327–329.
7. A. Taflove and S.C. Hagness, Computational electrodynamics: The finite-differecne time-domain method, 2nd ed., Artech House, Norwood, MA, 2000.
8. T. Namiki, A new FDTD algorithm based on alternating-direction implicit method, IEEE Trans Microwave Theory Tech 47 (1999), 2003–2007.
9. S. Ju, W. Yeo, and H. Kim, An efficient analysis of thin-film bulk acoustic wave resonators using FDTD method with ADI time-marching scheme, IEICE Trans Commun E88-B (2005), 2681–2684.
10. S.G. Garcia, T.W. Lee, and S.C. Hagness, On the accuracy of the ADI-FDTD method, IEEE Antennas Wireless Propag Lett 1 (2002), 31–34.
11. S. Wang, F.L. Teixeira, and J. Chen, An iterative ADI-FDTD with reduced splitting error, IEEE Microwave Wireless Compon Lett 15 (2005), 92–94.
12. G. Sun and C.W. Trueman, Unconditionally stable Crank-Nicolson scheme for solving two-dimensional Maxwell's equations, Electron Lett 30 (2003), 595–597.
13. R. Qiang, D. Wu, J. Chen, S. Wang, D. Wilton, and W. Kainz, An efficient two-dimensional FDTD method for bio-electromagnetic applications, IEEE Trans Magn 42 (2006), 1391–1394.
14. B.A. Auld, Acoustic fields and waves in solids, 2nd ed., Krieger, New York, 1990.

BODY SAR STUDY OF THE PLANAR WWAN MONOPOLE SLOT ANTENNA FOR TABLET DEVICE APPLICATION

Kin-Lu Wong and Wun-Jian Lin
Department of Electrical Engineering, National Sun Yat-Sen University, Kaohsiung 804, Taiwan; Corresponding author: wongkl@ema.ee.nsysu.edu.tw

Received 8 November 2010

ABSTRACT: *A study on the body SAR of the planar WWAN (wireless wide area network) monopole slot antenna for tablet device application is presented. The monopole slot antenna covers penta-band WWAN operation in the 824∼960/1710∼2170 MHz bands with low near-field emission such that its body SAR (specific absorption rate) values for 1-g tissue in the bottom face, landscape and portrait orientations to the flat phantom meet the limit of 1.6 W/kg for practical applications. Effects of the monopole slot antenna disposed at various possible locations in the tablet device on the body SAR results are also analyzed.* © 2011 Wiley Periodicals, Inc. Microwave Opt Technol Lett 53:1721–1727, 2011; View this article online at wileyonlinelibrary.com. DOI 10.1002/mop.26094

Key words: *mobile antennas; internal tablet device antennas; monopole slot antennas; WWAN antennas; Body SAR*

1. INTRODUCTION

Monopole slot antennas have the attractive feature of wideband operation and small size for internal mobile device antenna applications [1–9]. Their promising applications in the laptop computer for covering pentaband WWAN operation including the GSM850/900/1800/1900/UMTS bands (824∼894/880∼960/1710∼1880/1850∼1990/1920∼2170 MHz) have been shown [8, 9]. As such internal laptop computer antennas are mounted at the top edge of the display panel and generally have a distance of larger than 20 cm to the user's body, the SAR values of the antenna are not required to be tested [10–12]. However, for the tablet devices or tablet computers, whose configuration is of one-section slate type and is different from that of the traditional laptop computers, their internal antennas are mounted along the perimeter of the display panel of the tablet device and are generally with a small distance of less than 20 mm to the user's body in practical applications. Hence, the internal antennas for tablet device applications are required to be tested for the body SAR [10] and should meet the limit of 1.6 W/kg for 1-g tissue [11]. Presently, it is noted that there are no studies on the body SAR of the internal WWAN antennas reported in the published papers for tablet device applications.

In this article, we demonstrate that the planar monopole slot antennas are promising for application in the tablet devices to cover pentaband WWAN operation and meet the body SAR limit of 1.6 W/kg for 1-g tissue. The monopole slot antenna studied in this article has a planar structure and is easy to be printed on a thin dielectric substrate [9], making the antenna easy to fabricate at low cost. For the body SAR testing, the simulation model is introduced, and the simulated results are presented for analysis. Different testing models including the bottom face, landscape, and portrait conditions [10] for different orientations of the antenna to the flat phantom are studied. The obtained body SAR results for the antenna disposed at various possible locations in the tablet device are also analyzed.

2. WWAN MONOPOLE SLOT TABLET DEVICE ANTENNA

In this study, the planar WWAN monopole slot antenna used for tablet device application is shown in Figure 1. The antenna is printed on a 0.8-mm thick FR4 substrate of relative permittivity 4.4, loss tangent 0.024, and size 12×75 mm^2. The antenna comprises two monopole slots of different sizes (monopole slot 1 and 2 shown in the figure) that are successfully excited using a simple T-shape feeding strip. The antenna has been applied in a laptop computer as an internal WWAN antenna mounted at the center of the top edge of its 13-inch display panel (ground size 200×260 mm^2) [9]. The longer slot (monopole slot 1) generates a quarter-wavelength resonant mode at about 900 MHz for the antenna's lower band to cover the GSM850/900 operation (824∼960 MHz). The antenna's upper band is formed by two resonant modes, one being the higher-order resonant mode contributed by monopole slot 1 and the second being the quarter-wavelength resonant mode generated by the shorter slot (monopole slot 2).

Detailed operating principle of the studied monopole slot antenna has been presented in [9]. However, to be applied in a tablet device in which a 10-inch display panel with ground size 150×200 mm^2 is equipped therein, and the antenna is mounted along a shielding metal wall of width 5 mm, the dimensions of the studied monopole slot antenna need to be adjusted owing to the large ground plane difference when compared with that in [9]. The dimensions of the studied antenna are shown in the figure. Also note that the antenna is mounted at a location ($s = 10$ mm) close to one corner of the shielding metal wall such that along the shielding metal wall, there is still enough spacing to accommodate other possible internal antennas. The thickness of the tablet device is chosen to be 14 mm in this study (the dashed line indicates the housing of the tablet device). The

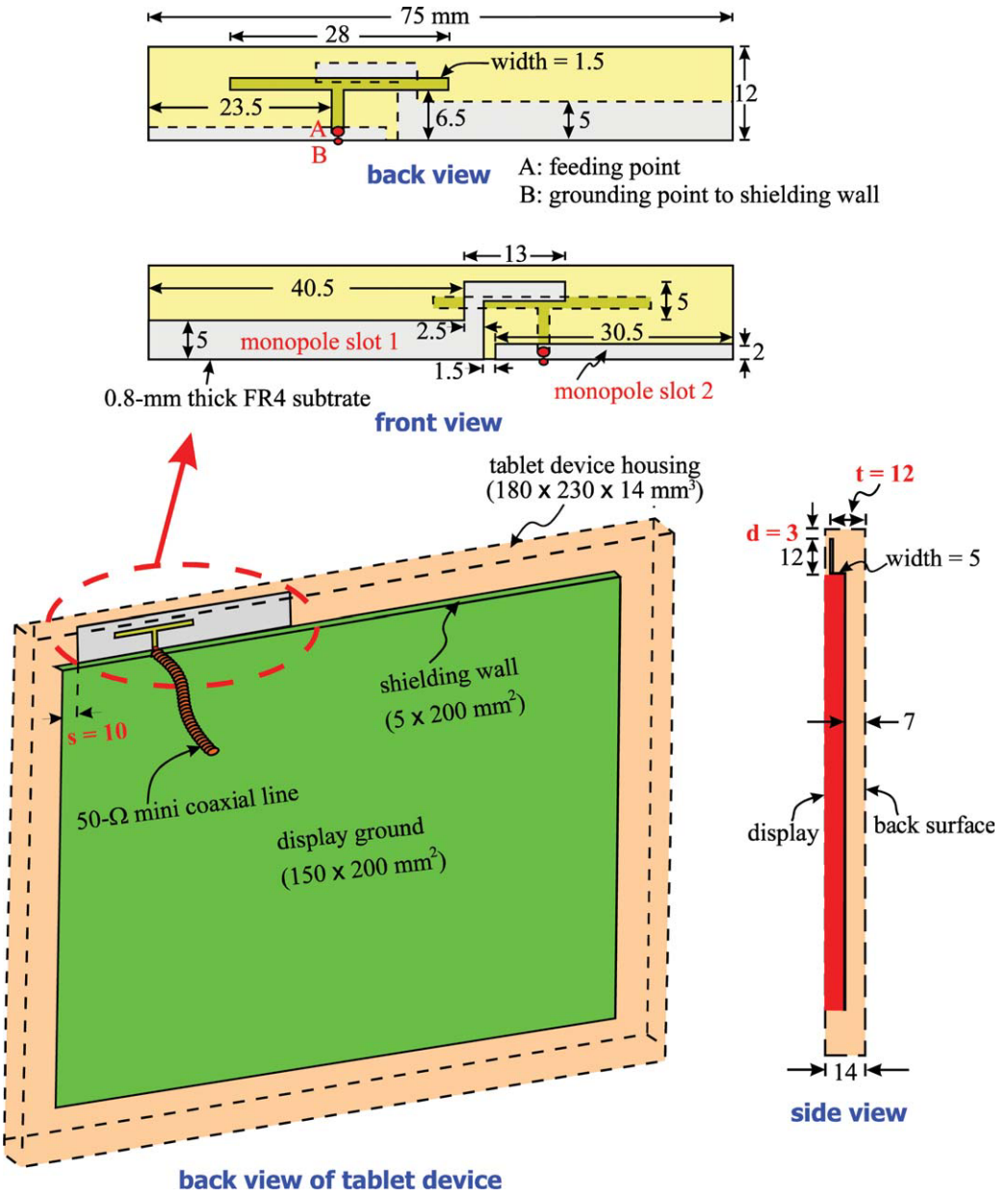

Figure 1 Geometry of the planar WWAN monopole slot antenna for tablet device application. [Color figure can be viewed in the online issue, which is available at wileyonlinelibrary.com]

antenna is mounted along the shielding metal wall and positioned at a location (t) 12 mm to the back surface of the tablet device. The spacing d between the top edge of the antenna and the top surface of the tablet device is 3 mm. In the region in-between the display ground and the back surface of the tablet device, it is for accommodating possible associated modules and electronic elements for the tablet device.

To confirm the selected dimensions of the studied antenna for covering pentaband WWAN operation, simulated results obtained using HFSS version 12 [13] and SEMCAD X version 14 [14] are first compared and shown in Figure 2. Good agreement between the two simulated results is seen. Further, the studied antenna is fabricated and tested. The measured results of the return loss are also in agreement with the simulated results using SEMCAD X shown in Figure 3. Over the five operating bands of GSM850/900/1800/1900/UMTS, the impedance matching is all better than 6-dB return loss. The simulated (SEMCAD

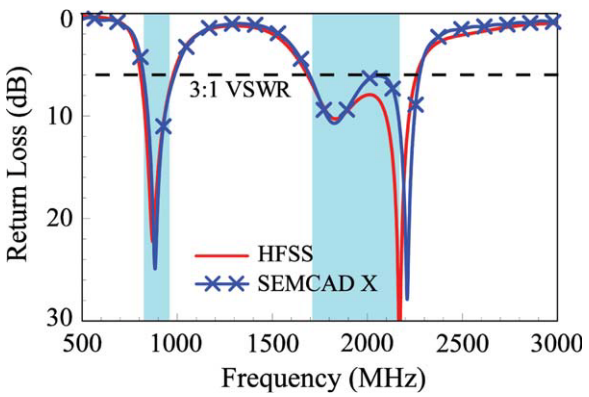

Figure 2 Comparison of the simulated return loss of the antenna obtained using HFSS and SEMCAD X simulation software. [Color figure can be viewed in the online issue, which is available at wileyonlinelibrary.com]

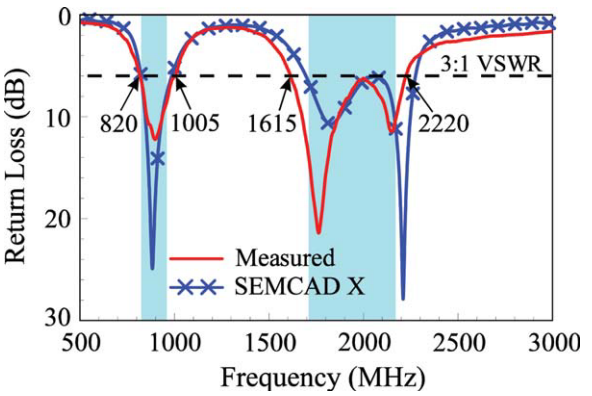

Figure 3 Measured and simulated return loss of the antenna. [Color figure can be viewed in the online issue, which is available at wileyonlinelibrary.com]

X) antenna efficiency that includes the mismatching loss of the antenna is also shown in Figure 4. The antenna efficiency is all larger than 60% over the WWAN bands, indicating that the studied antenna has good antenna efficiency for practical applications.

3. BODY SAR SIMULATION MODEL

Figures 5 and 6 show the body SAR simulation model for the antenna based on the simulation software SEMCAD X version 14 [14]. In the body SAR testing, a flat phantom shown in Figure 5 is used to simulate the human body [10]. The flat phantom is formed by filling a 2-mm thick plastic elliptic cylindrical container with tissue simulating liquid [15]. The parameters of both the plastic container and the tissue simulating liquid are given in the figure. According to the body SAR regulation [10], there are five conditions required to be tested. The first one is the bottom face condition in which the display is parallel to the flat phantom and the back surface of the tablet device is in direct contact against the flat phantom as shown in Figure 6(a). The other four conditions are related to the user-selectable display orientations (the display perpendicular to the flat phantom), which include two landscape conditions [primary and secondary landscape, see Fig. 6(b)] and two portrait conditions [primary and secondary portrait, see Fig. 6(c)]. Since the antennas in the secondary landscape and portrait conditions have a large distance (>100 mm) to the flat phantom, the obtained body SAR values for 1-g tissue

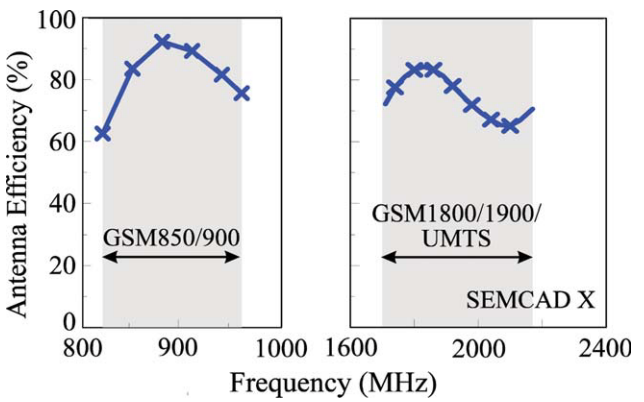

Figure 4 Simulated antenna efficiency (mismatching loss included) of the antenna. [Color figure can be viewed in the online issue, which is available at wileyonlinelibrary.com]

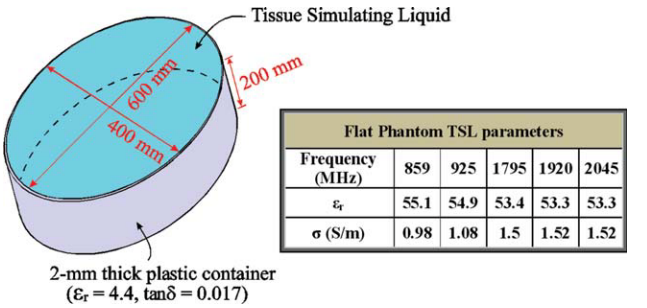

Flat Phantom TSL parameters					
Frequency (MHz)	859	925	1795	1920	2045
ε_r	55.1	54.9	53.4	53.3	53.3
σ (S/m)	0.98	1.08	1.5	1.52	1.52

Figure 5 Flat phantom for body SAR simulation model. [Color figure can be viewed in the online issue, which is available at wileyonlinelibrary.com]

are expected to be much less than the limit of 1.6 W/kg, and hence, the two conditions are skipped in the body SAR testing in this study. In the following section, the body SAR results for the three conditions of bottom face, primary landscape, and primary portrait are analyzed.

4. BODY SAR RESULTS

To begin with, the results of the simulated return loss for the antenna in free space and in the bottom face, primary landscape, and primary portrait conditions are presented in Figure 7. Although there are relatively large shiftings of the return loss in the lower band (GSM850/900) for the antenna in the primary landscape condition owing to the presence of the flat phantom, the impedance matching is still better than about 6-dB return loss. For the bottom face condition, some small degradation in the impedance matching for frequencies at about 2.1 GHz is seen; the impedance matching, however, is still better than about 5 dB. For the primary portrait condition, very small variations compared to that in free space are seen. This is largely because the antenna in the primary portrait condition has the largest distance to the flat phantom among the three different conditions.

Table 1 lists the obtained SAR values obtained using SEMCAD X for the antenna dimensions shown in Figure 1. The return loss at each testing frequency is also shown. The five frequencies at 859, 925, 1795, 1920, and 2045 MHz are the central frequencies of the five WWAN operating bands. The input power at each frequency is 0.25 Watt (24 dBm) at 859 and 925 MHz for GSM850/900 operation and 0.125 Watt (21 dBm) at 1795, 1920, and 2045 MHz for GSM1800/1900/UMTS operation. The input power is the same as that used for obtaining the head SAR for the internal handset antennas [16–22]. The SAR values for the three conditions all meet the limit of 1.6 W/kg. Note that the SAR value for the primary portrait condition is the lowest among the three conditions tested and is well below the limit of 1.6 W/kg. This is reasonable since the distance between the antenna and the flat phantom in the primary portrait condition is as large as 25 mm in this study, which is larger than 12 mm (t) in the bottom face condition and 3 mm (d) in the primary landscape condition.

Effects of the distance t in the bottom face condition and the distance d in the primary landscape condition are further analyzed. Figure 8 shows the body SAR results for the distance t varied from 8 to 12 mm in the bottom face condition. In this study, the distance (7 mm) between the display ground and the back surface of the tablet device is fixed. The decrease in the distance t is caused by moving the antenna on the shielding metal wall to be closer to the display ground, whereas other dimensions are the same as in Figure 1. The body SAR values

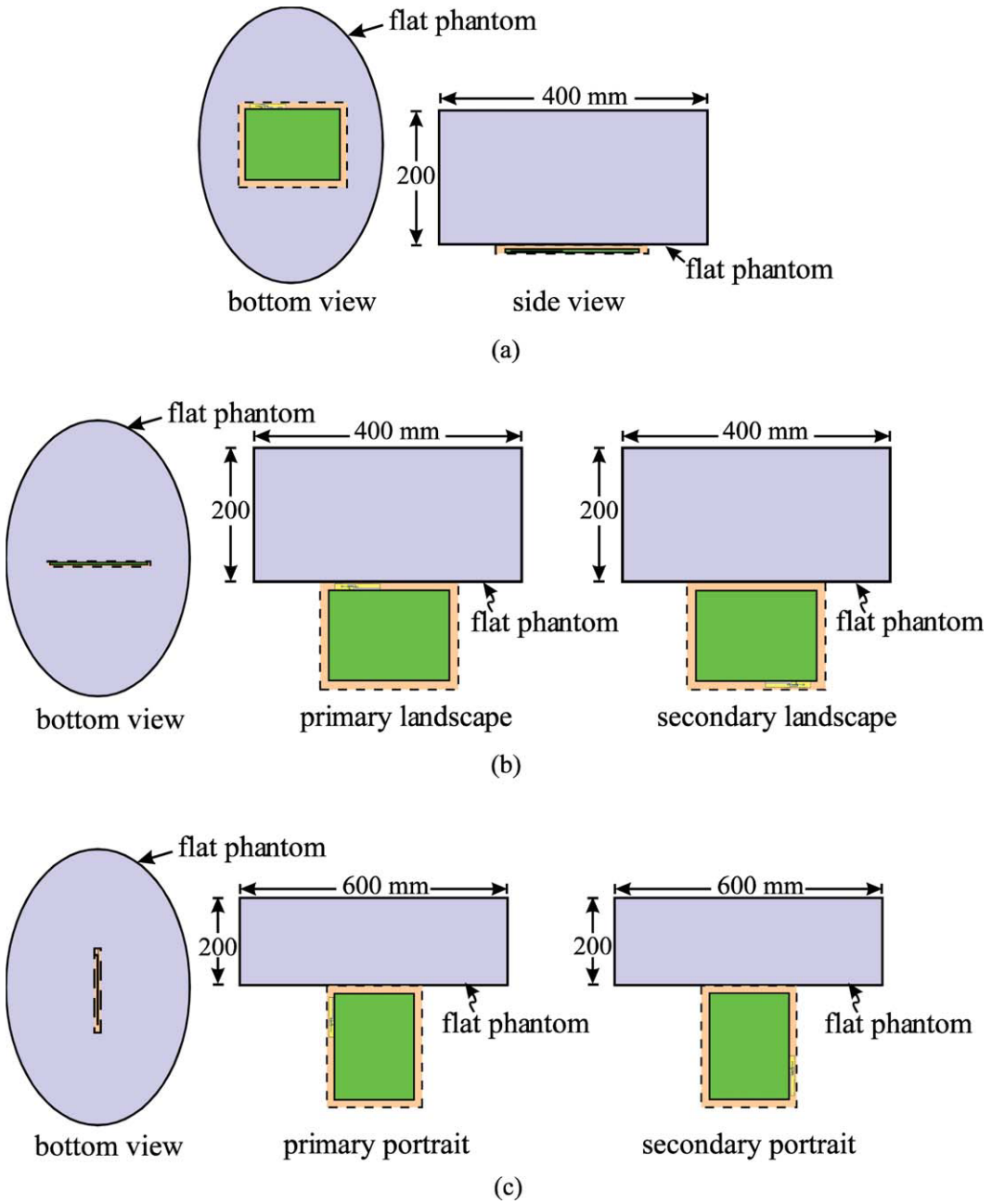

Figure 6 Body SAR simulation model for the antenna. (a) Bottom face condition. (b) Landscape condition. (c) Portrait condition. [Color figure can be viewed in the online issue, which is available at wileyonlinelibrary.com]

are in general increased with a decrease in the distance t. At 2045 MHz, large SAR value (2.06 W/kg) is seen for $t = 10$ mm. This is partly because the antenna is closer to the flat phantom and partly because the impedance matching is greatly enhanced to be 18.4 dB for $t = 10$ mm. The latter increases the near-field emission of the antenna and hence increases the SAR values. From the return loss shown in the figure, it also indicates that the impedance matching of the antenna is sensitive to its relative location in the tablet device and its distance to the flat phantom. For $t = 8$ mm, larger SAR values than 1.6 W/kg are observed (1.69 W/kg at 925 MHz and 2.0 W/kg at 1795 MHz), which makes the antenna fail to meet the 1-g SAR limit for practical applications.

Figure 9 shows the body SAR results for the distance d varied from 2 to 4 mm in the primary landscape condition. Other

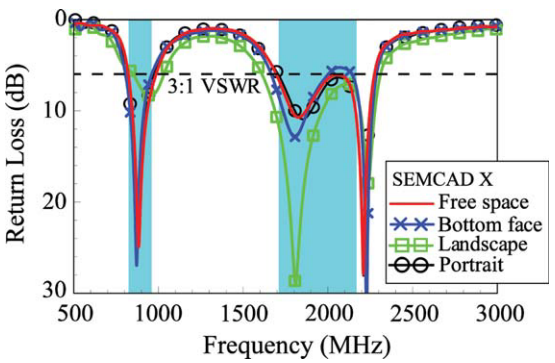

Figure 7 Comparison of the simulated return loss for the antenna in free space and in bottom face, primary landscape, and primary portrait conditions. [Color figure can be viewed in the online issue, which is available at wileyonlinelibrary.com]

TABLE 1 Body SAR Results of the Antenna for 1-g Tissue; t = 12 mm, d = 3 mm, s = 10 mm

Frequency (MHz)		859	925	1795	1920	2045
Input power (Watt)		0.25	0.25	0.125	0.125	0.125
1-g SAR (W/kg)	Bottom face	1.19	1.30	1.17	0.99	0.89
	Primary landscape	0.82	1.35	1.29	1.03	0.94
	Primary portrait	0.27	0.27	0.28	0.25	0.14
Return loss (dB)	Bottom face	19.9	8.9	13.5	8.6	5.8
	Primary landscape	6.5	8.2	25.1	12.7	7.9
	Primary portrait	16.9	10.2	9.9	9.9	6.9

The return loss shows the impedance matching level of the antenna at each testing frequency.

dimensions are the same as in Figure 1. In this case, relative location of the antenna in the tablet device is not changed. This also explains the observation that smaller variations are seen in the return loss when compared with that in the case in Figure 8. For d = 4 mm, smaller SAR values are seen, which is reasonable because the antenna has a larger distance to the flat phantom. For d = 2 mm, increased SAR values are seen. At 925 MHz, the SAR value is 1.62 W/kg, which exceeds the 1-g SAR limit for practical applications. At other frequencies, the SAR values still meet the limit of 1.6 W/kg.

Finally, the SAR results of the antenna as a function of the location s along the shielding metal wall of the display panel are studied. Results for the bottom face and primary landscape conditions are respectively shown in Figures 10(a) and 10(b). Again, since the relative location of the antenna along the shielding metal wall is changed for both conditions, the impedance matching is greatly varied as seen in the case in Figure. 8. Also note that for s = 62.5 mm, the antenna is located at about the center of the shielding metal wall. For the bottom face condition [Fig. 10(a)], the obtained SAR values all meet the limit of 1.6 W/kg. This suggests that for the bottom face condition, the distance t between the antenna and the flat phantom is the most important factor in the body SAR.

For the primary landscape condition [Fig. 10(b)], large variations in the body SAR for different values of s are seen. The body SAR variations are also much larger than that seen in the bottom face condition in Figure 10(a). However, it is interesting to note that the body SAR values for s = 62.5 mm are the smallest among the three different locations. This may be attributed to the condition that the antenna in the case of s = 62.5 mm is generally symmetric with respect to the display ground, which may result in more smooth surface current distributions excited on the shielding metal wall and the display ground. This leads to a decrease in the strength of the total near-field emis-

Bottom face						
Frequency (MHz)		859	925	1795	1920	2045
1-g SAR (W/kg)	t = 12 mm	1.19	1.30	1.17	0.99	0.89
	t = 10 mm	1.14	1.60	1.58	1.44	2.06
	t = 8 mm	1.38	1.69	2.00	1.51	1.41
Return loss (dB)	t = 12 mm	19.9	8.9	13.5	8.6	5.8
	t = 10 mm	10.0	11.7	9.9	26.1	18.4
	t = 8 mm	10.6	7.3	18.4	9.8	6.5

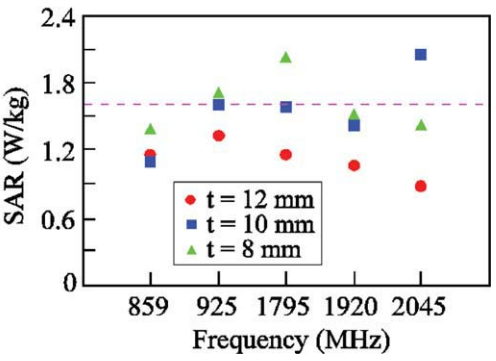

Figure 8 Body SAR values as a function of the distance t between the antenna and the flat phantom in the bottom face condition. Other dimensions are the same as in Figure 1. [Color figure can be viewed in the online issue, which is available at wileyonlinelibrary.com]

Primary landscape						
Frequency (MHz)		859	925	1795	1920	2045
1-g SAR (W/kg)	d = 2 mm	0.96	1.62	1.41	1.17	1.07
	d = 3 mm	0.82	1.35	1.29	1.03	0.94
	d = 4 mm	0.81	1.37	1.33	1.01	0.93
Return loss (dB)	d = 2 mm	5.8	7.1	34.9	11.6	7.6
	d = 3 mm	6.5	8.2	25.1	12.7	7.9
	d = 4 mm	6.7	8.8	22.1	12.9	8.0

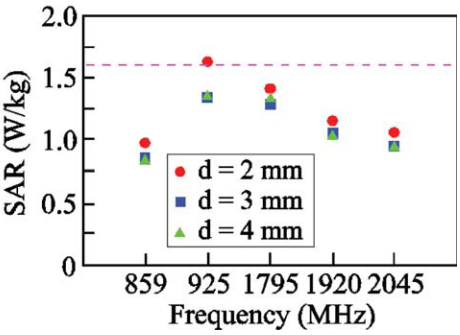

Figure 9 Body SAR values as a function of the distance d between the antenna and the flat phantom in the primary landscape condition. Other dimensions are the same as in Figure 1. [Color figure can be viewed in the online issue, which is available at wileyonlinelibrary.com]

Bottom face						
Frequency (MHz)		859	925	1795	1920	2045
1-g SAR (W/kg)	s = 10.0 mm	1.19	1.30	1.17	0.99	0.89
	s = 36.0 mm	1.45	1.54	1.11	0.86	0.85
	s = 62.5 mm	1.48	1.48	1.36	0.98	0.78
Return loss (dB)	s = 10.0 mm	19.9	8.9	13.5	8.6	5.8
	s = 36.0 mm	13.7	7.3	25.0	10.5	12.4
	s = 62.5 mm	18.5	7.1	17.2	8.6	6.1

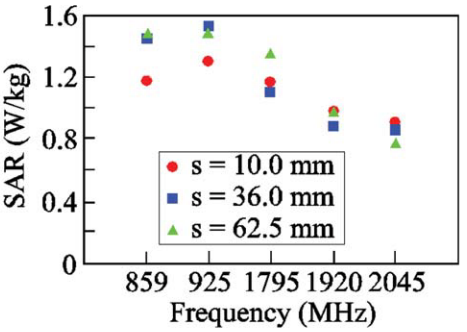

(a)

Primary landscape						
Frequency (MHz)		859	925	1795	1920	2045
1-g SAR (W/kg)	s = 10.0 mm	0.82	1.35	1.29	1.03	0.94
	s = 36.0 mm	1.42	1.50	1.90	1.22	0.90
	s = 62.5 mm	0.47	0.73	1.20	0.77	0.71
Return loss (dB)	s = 10.0 mm	6.5	8.2	25.1	12.7	7.9
	s = 36.0 mm	6.7	4.3	14.3	14.0	15.1
	s = 62.5 mm	9.5	7.5	12.6	9.7	10.0

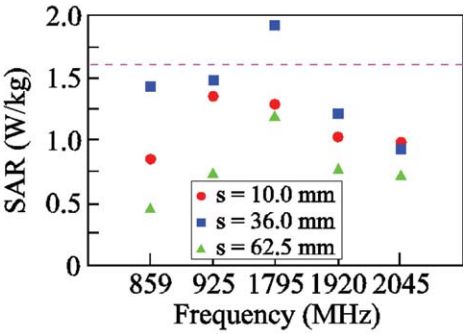

(b)

Figure 10 Body SAR values as a function of the location *s* along the shielding wall of the display panel. (a) Bottom face condition. (b) Primary landscape condition. Other dimensions are the same as in Figure 1. [Color figure can be viewed in the online issue, which is available at wileyonlinelibrary.com]

sion of the tablet device in the flat phantom, which results in decreased body SAR values.

5. CONCLUSIONS

The body SAR results of a planar WWAN monopole slot antenna suitable for tablet device applications have been presented and analyzed. As the WWAN monopole slot antenna has a two-dimensional planar structure, the distance between the antenna in the tablet device and the flat phantom in the bottom face condition can be maximized. This distance (t in Fig. 1) has been shown to be an important factor in the body SAR for the bottom face condition. To meet the 1-g SAR limit of 1.6 W/kg, the distance t is required to be 12 mm in this study. For the primary landscape condition, the distance (d in Fig. 1) between the antenna and the flat phantom is also an important factor. In addition, the relative location (s in Fig. 1) of the antenna with respect to the display ground is also important in achieving decreased body SAR values. For the primary portrait condition, since the antenna has a large distance of 25 mm to the flat phantom, small SAR values in this condition are obtained. The obtained results indicate that it is very promising for the planar WWAN monopole slot antenna to be applied in the tablet device to meet the body SAR regulation required for practical applications.

REFERENCES

1. H. Wang, M. Zheng, and S.Q. Zhang, Monopole slot antenna, U.S. Patent No. 6,618,020 B2, Sep. 9, 2003.
2. P. Lindberg, E. Ojefors, and A. Rydberg, Wideband slot antenna for low-profile hand-held terminal applications, Proc 36th European Microwave Conf (EuMC2006), Manchester, UK, 2006. pp. 1698–1701.
3. C.I. Lin and K.L. Wong, Printed monopole slot antenna for internal multiband mobile phone antenna, IEEE Trans Antennas Propagat 55 (2007), 3690–3697.
4. C.H. Wu and K.L. Wong, Hexa-band internal printed slot antenna for mobile phone application, Microwave Opt Technol Lett 50 (2008), 35–38.
5. C.H. Chang and K.L. Wong, Internal multiband surface-mount monopole slot chip antenna for mobile phone application, Microwave Opt Technol Lett 50 (2008), 1273–1279.
6. C.I. Lin and K.L. Wong, Printed monopole slot antenna for penta-band operation in the folder-type mobile phone, Microwave Opt Technol Lett 50 (2008), 2237–2241.
7. F.H. Chu and K.L. Wong, Simple folded monopole slot antenna for penta-band clamshell mobile phone application, IEEE Trans Antennas Propagat 57 (2009), 3680–3684.
8. K.L. Wong and L.C. Lee, Multiband printed monopole slot antenna for WWAN operation in the laptop computer, IEEE Trans Antennas Propagat 57 (2009), 324–330.
9. K.L. Wong and F.H. Chu, Internal planar WWAN laptop computer antenna using monopole slot elements, Microwave Opt Technol Lett 51 (2009), 1274–1279.
10. Federal Communications Commission, Office of Engineering and Technology, Mobile and Portable Device RF Exposure Equipment Authorization Procedures, OET/Lab Knowledge Database publication number 447498 item 7, Dec. 13, 2007.
11. American National Standards Institute (ANSI), Safety levels with respect to human exposure to radio frequency electromagnetic fields, 3 kHz to 300 GHz, ANSI/IEEE standard C95.1, April 1999.
12. IEC 62209–1, Human exposure to radio frequency fields from hand-held and body-mounted wireless communication devices—

Human models, instrumentation, and procedures—Part 1: Procedure to determine the specific absorption rate (SAR) for hand-held devices used in close proximity to the ear (frequency range of 300 MHz to 3 GHz), Feb. 2005.
13. http://www.ansoft.com/products/hf/hfss/, Ansoft Corporation HFSS.
14. http://www.semcad.com, SPEAG SEMCAD, Schmid & Partner Engineering AG.
15. http://www.ntt-at.com/products_e/sar/index.html, Tissue Simulating Liquid for SAR Measurement, NTT Advanced Technology Corporation.
16. F.H. Chu and K.L. Wong, Simple planar printed strip monopole with a closely-coupled parasitic shorted strip for eight-band LTE/GSM/UMTS mobile phone, IEEE Trans Antennas Propagat 58 (2010), 3426–3431.
17. K.L. Wong and S.C. Chen, Printed single-strip monopole using a chip inductor for penta-band WWAN operation in the mobile phone, IEEE Trans Antennas Propagat 58 (2010), 1011–1014.
18. C.T. Lee and K.L. Wong, Internal WWAN clamshell mobile phone antenna using a current trap for reduced groundplane effects, IEEE Trans Antennas Propagat 57 (2009), 3303–3308.
19. Y.W. Chi and K.L. Wong, Quarter-wavelength printed loop antenna with an internal printed matching circuit for GSM/DCS/PCS/UMTS operation in the mobile phone, IEEE Trans Antennas Propagat 57 (2009), 2541–2547.
20. C.H. Chang and K.L. Wong, Printed λ/8-PIFA for penta-band WWAN operation in the mobile phone, IEEE Trans Antennas Propagat 57 (2009), 1373–1381.
21. K.L. Wong, W.Y. Chen, C.Y. Wu, and W.Y. Li, Small-size internal eight-band LTE/WWAN mobile phone antenna with internal distributed LC matching circuit, Microwave Opt Technol Lett 52 (2010), 2244–2250.
22. S.C. Chen and K.L. Wong, Bandwidth enhancement of coupled-fed on-board printed PIFA using bypass radiating strip for eight-band LTE/GSM/UMTS slim mobile phone, Microwave Opt Technol Lett 52 (2010), 2059–2065.

NOVEL SERIES-FED MICROSTRIP ARRAY ANTENNA WITH MINIATURIZED FEEDING NETWORK FOR WLAN/RFID APPLICATIONS

Chia-Hao Ku,[1] Hsien-Wen Liu,[2] and Yu-Shu Lin[2]
[1] Department of Electrical Engineering, Ming Chi University of Technology, Taipei, Taiwan, Republic of China
[2] Department of Electrical Engineering, National Taiwan University of Science and Technology, Taipei, Taiwan, Republic of China; Corresponding author: D9407303@mail.ntust.edu.tw

Received 16 October 2010

ABSTRACT: *A novel series-fed microstrip array antenna with a miniaturized feeding network suitable for wireless local area network (WLAN) and radio frequency identification (RFID) applications is presented. This array works with 10 patch elements and utilizes artificial transmission lines (ATL) to design the feeding network to well reduce the whole size. Compared to conventional series-fed array designs, the proposed array can achieve not only a small size of merely 14 (*L*) × 230 (*W*) mm*^{2} *but also a wide operating bandwidth from 5 to 5.94 GHz. Experimental results exhibit that fairly good broadside radiation pattern with adequate half-power beamwidth for practical application can be obtained with our array design. Therefore, the proposed microstrip array antenna with a compact size is well suitable to be integrated within the WLAN/RFID systems as a transmitting antenna.* © 2011 Wiley Periodicals, Inc. Microwave Opt Technol Lett 53:1727–1730, 2011; View this article online at wileyonlinelibrary.com. DOI 10.1002/mop.26120

Key words: *series-fed microstrip array antenna; artificial transmission line; half-power beamwidth; WLAN; RFID*

1. INTRODUCTION

In recent years, microstrip array antennas with several attractive advantages such as low cost and easy fabrication have been widely utilized for various communication systems as a transmitting antenna. For achieving better communication quality, the microstrip array antenna must be developed with adequate operating bandwidth as well as wide half-power beamwidth to meet practical application. To this end, many array antenna designs have been devoted to tackling different demands [1–6]. Two array antennas using U-shaped slot to broaden the operating bandwidth were reported in [1, 2]. By properly using L-probe [3], tooth-like-slot [4], and inverted feeding structure [5], the beamwidth of the patch array could be widened to cover a large communication area. To have a compact array size, on the other hand, a taper array antenna with series-fed structure was also discussed in [6]. However, these prior array designs cannot achieve all desirable characteristics including compact size, wideband operation, and large coverage for practical application.

In this letter, we, thus, propose a compact printed series-fed 1 × 10 microstrip array antenna for wireless local area network (WLAN: 5.725–5.85 GHz) and radio frequency identification (RFID: 5.725–5.875 GHz) operations. This array is consisted of 10 radiating elements and a miniaturized feeding network. By properly using artificial transmission lines (ATL) to construct the feeding network, the array size can be reduced significantly. Compared with previous array designs presented in [1–6], the proposed array antenna behaves not only a more compact size of merely 14 (L) × 230 (W) mm^2 to be easily integrated into the WLAN/RFID systems as a transmitting antenna but also a wide operating bandwidth from 5 to 5.94 GHz. Properties such as high antenna gain and good sidelobe level (SLL) over the operating frequency band are also obtained with our array design. Hence, the proposed patch array, with enough half-power beamwidth to enlarge the service range, is well satisfactory for WLAN/RFID operations. Details of the array design are then described in Section 2, and a fabricated prototype of the array is also tested and analyzed in Section 3. Parameters regarding half-power beamwidth and SLL are carefully tabulated

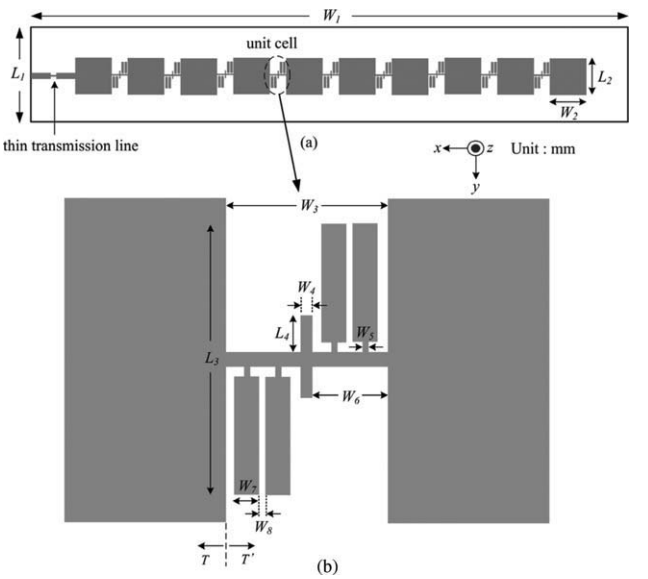

Figure 1 Geometry of the proposed series-fed microstrip array antenna. (L_1 = 14 mm, L_2 = 14 mm, L_3 = 9.9 mm, L_4 = 1.4 mm, W_1 = 230 mm, W_2 = 14 mm, W_3 = 6.4 mm, W_4 = 0.5 mm, W_5 = 0.2 mm, W_6 = 2.8 mm, W_7 = 0.9 mm, and W_8 = 0.2 mm)